Eur. Phys. J. A **16**, 313–329 (2003)
DOI 10.1140/epja/i2002-10105-x

THE EUROPEAN PHYSICAL JOURNAL A

Beta-decay of the N = Z nucleus ^{72}Kr

I. Piqueras[1,2], M.J.G. Borge[1,a], Ph. Dessagne[2], J. Giovinazzo[2,b], A. Huck[2], A. Jokinen[3], A. Knipper[2], C. Longour[2], G. Marguier[4], M. Ramdhane[3,c], V. Rauch[2], O. Tengblad[1,3], G. Walter[2], Ch. Miehé[2], and the ISOLDE Collaboration[3]

[1] Instituto de Estructura de la Materia, CSIC, Serrano 113bis, E-28006 Madrid, Spain
[2] Institut de Recherches Subatomiques, UMR 7500 CNRS-IN2P3 et Université Louis Pasteur, 23 rue du Loess, B.P. 28, F-67037 Strasbourg Cedex 2, France
[3] ISOLDE, Division EP, CERN CH-1211 Geneva, Switzerland
[4] Institut de Physique Nucléaire, Université Claude Bernard-Lyon I, F-69622 Villeurbanne Cedex, France

Received: 7 February 2002 / Revised version: 14 October 2002 /
Published online: 6 March 2003 –
Communicated by J. Äystö

Dedicated to Christiane Miehé on her 60th Birthday

Abstract. The beta-decay of the $N = Z$, even-even nucleus ^{72}Kr has been studied at the ISOLDE PSB facility at CERN. Measurements of $\beta\gamma$ and $\beta\gamma\gamma$ coincidences have enriched the decay scheme of the daughter nucleus ^{72}Br with 27 new low spin levels. A more precise half-life of $T_{1/2} = 17.1(2)$ s has been determined. Strong feeding to the ^{72}Br ground state is established yielding an unambiguous $J^\pi = 1^+$ assignment for this state. Candidates for the ^{72}Br g.s. wave function are discussed in the framework of a self-consistent deformed mean-field calculation with SG2 Skyrme force and pairing correlations. A search for beta-delayed particle emission was made and an upper limit of 10^{-6} for this decay branch obtained. The cumulated experimental level density of 1^+ states has been fitted with the *constant temperature formula*. The comparison indicates that most likely all 1^+ levels up to 1.2 MeV have been observed in this investigation. The corresponding nearest-neighbour level spacing does not follow a Poisson distribution. The Gamow-Teller strength distribution is compared, in terms of nuclear deformation, with different calculations made in the framework of the quasiparticle random phase approximation.

PACS. 21.10.Hw Spin, parity, and isobaric spin – 23.20.Lv Gamma transitions and level energies – 23.40.Hc Relation with nuclear matrix elements and nuclear structure – 27.50.+e $59 \leq A \leq 89$

1 Introduction

Far from stability, studies of Gamow-Teller (GT) beta-decay are often the main way to investigate nuclear structure, since it offers unparalleled access to low-spin states over a large energy range. Measurements of the total GT strength and its distribution over the $Q_{\rm EC}$ window are of great interest for comparison with different theoretical descriptions. For even-even $N = Z$ nuclei the GT process is the only *allowed* decay mode. The structure of these nuclei is of special interest because one expects proton-neutron correlations to play a particularly important role. It is also well known from both experiment and theory that in neutron-deficient nuclei near $A = 70$ both shape transitions and shape coexistence occur.

Renewed interest in β-decay studies of the $A \approx 70$ nuclei has come from the recent theoretical breakthrough made by Hamamoto *et al.* [1,2], and the subsequent work of Sarriguren *et al.* [3]. Their results indicate that it is of interest not only to explore the properties of the excited states, but also the radioactive decay of these nuclei, as information on the ground-state (g.s.) deformation can be obtained in this particular region from the GT strength distribution. In studies of the decay of the even-even nuclei one obtains information not only on the parent ground state, but also on the level structure at low excitation energy and low spin in the odd-odd daughter nucleus. In particular one obtains information on the 1^+ states fed by allowed transitions.

[a] e-mail: borge@pinar2.csic.es
[b] *Present address*: Centre d' Etudes Nucléaires de Bordeaux-Gradignan, Le Haut Vigneau, F-33175 Gradignan Cedex, France.
[c] *Present address*: University Mentouri, 25000 Constantine, Algeria.

As part of a systematic study of the β^+-EC decay of $N = Z$ nuclei in the $A = 72$–80 deformed region, a study of the β-decays of ^{72}Kr and ^{76}Sr has been undertaken. Preliminary results have been presented in [4–6]. In this paper the detailed study of the β^+-EC decay of ^{72}Kr is reported. This study benefits greatly of the high production yields and selectivity of the ISOLDE/CERN mass separator. Previous studies by Schmeing *et al.* [7], and Davids and Goosman [8] established seven γ-lines following the β-decay. In both works the resulting level schemes placed four 1^+ excited states up to 0.58 MeV in ^{72}Br, and the g.s.-to-g.s. transition was measured. The latter measurement suggested $J^\pi = 1^+$ for the ^{72}Br (g.s.). This is inconsistent with the 3^+ assignment suggested by the decay study of the ^{72}Br daughter [9], leaving the question of the spin of the ^{72}Br ground state open. Later analysis of in-beam γ-ray measurements [10–12] based a positive-parity band on the $J^\pi = 3^+$ value.

In order to exploit the full $Q_{\rm EC}$ window ($Q_{\rm EC} = 5040$ (80) keV [13]), our γ-ray spectroscopy studies were combined with a careful search for delayed particle emission, which is expected from systematics ($S_{\rm p} = 3350$ (327) keV [13]).

2 Experimental setup

The experiment was performed at the ISOLDE facility [14] at CERN, Geneva, Switzerland. The ^{72}Kr ion beam was produced in the reaction of a 3×10^{13}/pulse 1 GeV proton beam, delivered by the CERN-PSB, with a 37 g/cm^2 Nb-foil target. During the experiment the target received six of the twelve proton pulses produced per 14.4 second supercycle. The average ^{72}Kr yield was 2×10^3 atoms/μC. The separation efficiency, given as released fraction (0.45) $\times$ transport efficiency (0.88) $\times$ Kr ionization efficiency, was $7.9(4) \times 10^{-3}$. After separation, the produced Kr ions were collected on an aluminized Mylar tape connecting two counting stations, which were used in parallel.

In order to suppress isobaric contaminants, especially directly produced bromine, the transfer line between the target chamber and the plasma ion source was water cooled. To determine the efficiency of this procedure, data on the well-known ^{73}Kr decay [15] was collected at $A = 73$ under the same conditions. The isobaric contamination at $A = 73$, and therefore also at $A = 72$, was found to be negligible, corresponding to a suppression factor of more than 10^4.

The bottom station, where the radioactive beam was collected, was dedicated to $\beta\gamma\gamma$ coincidence measurements. Two HPGe detectors of 70% and 80% efficiency, each covering a solid angle of 5% of 4π, were placed facing the collection point. Both detector signals were recorded in coincidence with those of a $4\pi\beta$-detector of 80% efficiency surrounding the collection point. The dynamic energy ranges of the HPGe detectors were 20–1000 keV and 90–4500 keV, respectively, allowing the study of a large region of the $Q_{\rm EC}$ window with good energy resolution.

A second station, called upper station, was situated above the collection point and connected to it by a tape transport system. It was equipped with a gas-Si telescope with low energy threshold specially designed to observe beta-delayed proton emission and with a high-efficiency HPGe γ-counter and a Si(Li) detector for low-energy γ-rays. The proton telescope, which covered a solid angle of 20% of 4π consisted of an ultra-thin gas ΔE counter backed by a 1134 mm^2, 500 μm thick silicon detector. A 92(2) μg/cm^2 polypropylene entrance window separated the gas counter, with a pressure of 20 torr of continuously circulating isobutane, from the beam line vacuum system. The calibration of the particle spectra was performed with the alpha emitters ^{239}Pu, ^{241}Am, ^{244}Cu and the conversion electron emitter ^{207}Bi. The γ-counter was an 80% efficient HPGe detector, covering 5% of 4π and an energy range of 70–4700 keV. The Si(Li) low-energy γ-ray detector covered energies up to 100 keV and 15% of 4π solid angle. This device allows direct γ-ray studies as well as particle-γ and γ-low energy-γ coincidences to be recorded. As the activity is deposited on the tape and moved to the second station, this measuring point is free from built-up activity in the surrounding materials and therefore better suited to extract the half-life from the temporal behaviour of the observed γ-lines and to determine the ground-state feeding.

The gamma spectra were recorded in singles and multispectra modes in order to obtain information about intensities and half-lives. The time cycle was 28 s for the collection and measurement at the bottom station, with a transport time of 200 ms to move the sample to the upper station and an identical time of 28 s for the measurement time at the upper one. Every measurement was

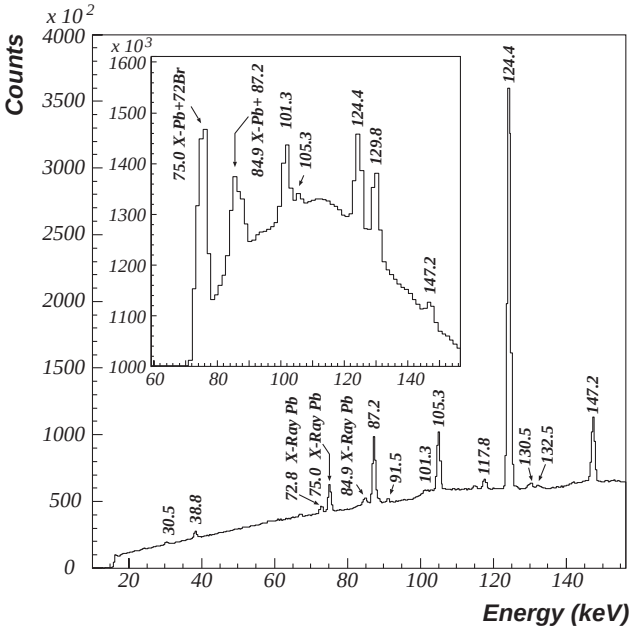

Fig. 1. Low-energy β-gated gamma spectrum registered at the bottom station with the 70% HPGe detector during 25.8 h. The inset presents the γ-ray spectrum taken with the 80% HPGe detector in the upper station, for the same energy interval and equal period of time. Note the difference in relative intensities of the 101.3 and 124.4 keV γ-rays between the two stations.

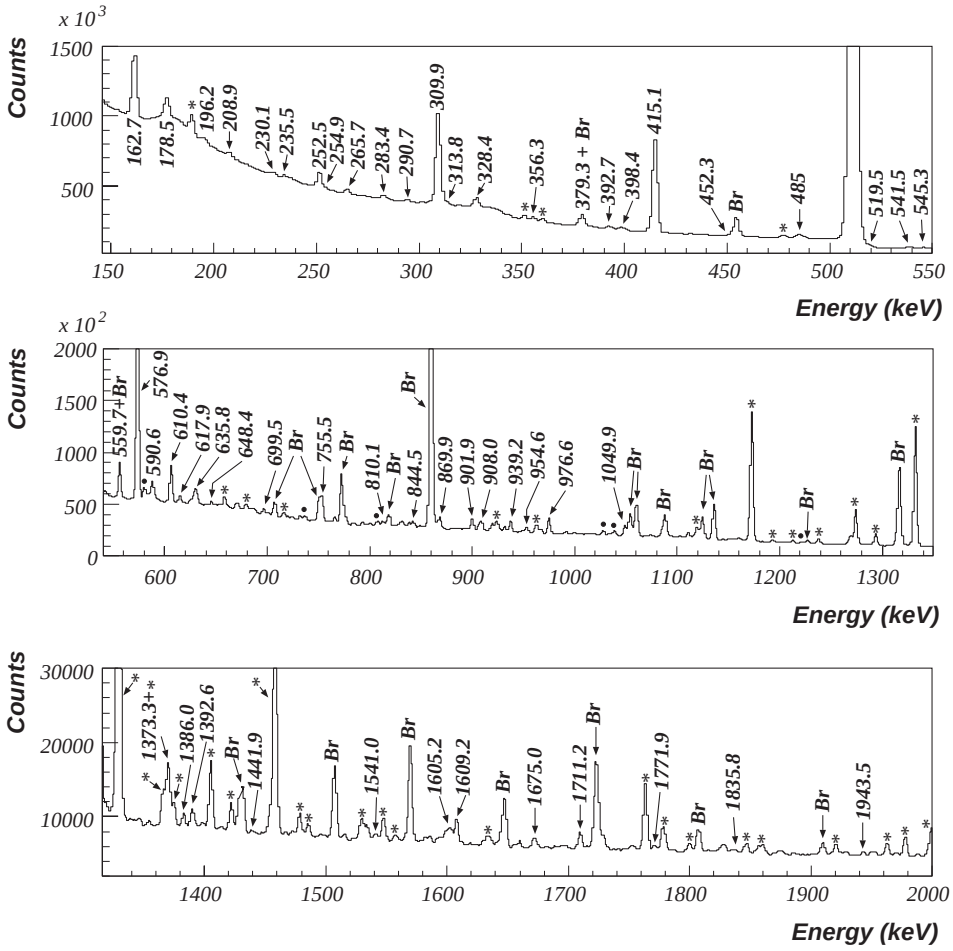

Fig. 2. Gamma spectrum in the energy range 150–2000 keV registered at the upper station. The peaks labeled with energies or with solid black circles correspond to transitions attributed to the ^{72}Kr decay (see table 1 for a complete listing). The lines marked with Br belong to the decay of ^{72}Br [17]. The asterisk indicates lines from background activities.

divided into eight time bins of 3.5 s each to investigate the temporal behaviour of the γ-rays.

3 Analysis and results

3.1 Gamma-ray spectroscopy

The low-energy part of the γ-ray spectra is shown in fig. 1. The β-gated spectrum from the bottom station is displayed up to 150 keV and in the inset the singles γ-spectrum obtained for the same energy range in the upper station. The singles γ-spectrum obtained in the upper station from 150 keV upwards is shown in fig. 2. In table 1 we list the energies, relative intensities and assignments of the γ-lines attributed to ^{72}Br following the β^+ decay of ^{72}Kr. The assignment of a γ-line to the ^{72}Kr decay was made on the basis of fulfillment of one or both of the two following criteria. First, a γ-ray was attributed to the decay if the temporal behaviour of the intensity in the different subgroups corresponded to the expected $T_{1/2}$. By this method 35 new γ-lines were identified as belonging to the decay of ^{72}Kr. In the case of unresolved doublets, we studied the evolution of the centroid position. If both peaks belong to the same decay, the position of the centroid is the same in all the eight bins. However, if one of the γ-lines is from the ^{72}Kr decay and the other is a long-lived contaminant or from the decay of a daughter nucleus, an appreciable variation in the doublet shape and a shift of the centroid with time are observed. Secondly, the assignment was made on the basis of a study of $\gamma\gamma$ coincidence data.

In order to determine the relative intensities of the γ-lines the results of the three HPGe detectors were compared and the weighted mean was calculated, unless the values differed considerably. As this was in most cases due to the presence of unresolved peaks, the value obtained from the detector with the best energy resolution was chosen.

One should notice that the intensities of γ-lines up to 320 keV have been corrected for internal conversion. The transition multipolarities were taken either from previous in-beam measurements [10,11] or from our new spin assignments. The calculated conversion coefficients were taken from ref. [16]. The extracted relative intensities ($I_{\gamma+\mathrm{IC}} = I_\gamma \times (1 + \alpha)$) for the transitions are listed in table 1.

Table 1. Gamma transitions in the decay of ^{72}Kr.

E_γ (keV)	$I^{(a)}_{\gamma+IC}$	E_i (keV)	E_f (keV)
30.5 ± 0.5	23.99 ± 4.13	131.8	101.3
38.8 ± 0.2	2.99 ± 0.69	162.8	124.4
87.2 ± 0.5	6.15 ± 0.86	218.9	131.8
88.5 ± 0.5	0.56 ± 0.48	398.5	310.0
91.5 ± 0.5	0.33 ± 0.07	310.0	218.9
101.3 ± 0.3	33.07 ± 4.06	101.3	0
105.3 ± 0.1	3.39 ± 0.33	415.2	310.0
117.8 ± 0.5	0.55 ± 0.13	218.9	101.3
124.4 ± 0.2	31.15 ± 2.76	124.4	0
130.5 ± 0.5	0.73 ± 0.12	509.9	379.3
132.5 ± 0.5	0.23 ± 0.04	708.3	575.9
146.2 ± 0.4	0.14 ± 0.10	722.3	575.9
147.2 ± 0.1	3.52 ± 0.32	310.0	162.8
147.2 ± 0.1	0.60 ± 0.23	545.7	398.5
160.8 ± 0.6	0.70 ± 0.08	575.9	415.2
162.7 ± 0.1	68.95 ± 5.58	162.8	0
166.1 ± 0.7	0.72 ± 0.14	328.6	162.8
177.2 ± 0.5	0.88 ± 0.08	575.9	398.5
178.5 ± 0.5	16.32 ± 1.33	310.0	131.8
183.3 ± 0.5	1.80 ± 0.22	575.9	392.8
185.5 ± 0.7	0.18 ± 0.11	310.0	124.4
196.2 ± 0.5	2.34 ± 0.82	415.2	218.9
196.2 ± 0.5	1.11 ± 0.55	509.9	313.8
199.8 ± 0.5		509.9	310.0
204.4 ± 0.2	0.66 ± 0.12	328.6	124.4
208.9 ± 0.3	4.22 ± 0.33	310.0	101.3
218.8 ± 0.5	0.38 ± 0.14	218.9	0
230.1 ± 0.3	2.38 ± 0.18	392.8	162.8
$231.8^{(b)} \pm 0.3$		545.7	313.8
235.5 ± 0.4	3.24 ± 0.24	545.7	310.0
252.4 ± 0.2	15.51 ± 0.50	415.2	162.8
254.9 ± 0.5	1.23 ± 0.09	379.3	124.4
265.7 ± 0.2	3.06 ± 0.15	575.9	310.0
267.0 ± 0.5	0.55 ± 0.14	398.5	131.8
274.2 ± 0.3	1.21 ± 0.07	398.5	124.4
283.4 ± 0.4	4.78 ± 0.13	415.2	131.8
290.7 ± 0.4	0.31 ± 0.06	415.2	124.4
307.0 ± 0.5	1.16 ± 0.11	722.3	415.2
309.9 ± 0.1	100.0 ± 1.54	310.0	0
313.8 ± 0.3	3.63 ± 0.11	313.8	0
328.4 ± 0.2	7.60 ± 0.24	328.6	0
356.3 ± 0.5	0.56 ± 0.04	902.3	545.7
379.3 ± 0.5	5.24 ± 0.97	379.3	0
379.3 ± 0.5	0.13 ± 0.02	708.3	328.6
380.8 ± 0.2	3.89 ± 0.16	796.1	415.2
385.4 ± 0.5	0.44 ± 0.06	509.9	124.4
392.7 ± 0.2	3.75 ± 0.13	392.8	0
398.4 ± 0.2	3.61 ± 0.17	398.5	0
412.1 ± 0.2	2.35 ± 0.08	722.3	310.0
414.5 ± 0.5	41.14 ± 4.02	577.0	162.8
415.1 ± 0.2	83.55 ± 4.62	415.2	0
427.1 ± 0.3	0.48 ± 0.05	755.7	328.6
451.4 ± 0.5	1.02 ± 0.20	1027.9	575.9
452.3 ± 0.3	4.63 ± 0.17	577.0	124.4
482.5 ± 0.5	0.82 ± 0.20	1027.9	545.7
484.7 ± 0.5	2.75 ± 0.22	1386.4	902.3
485.9 ± 0.5	2.82 ± 0.08	796.1	310.0

Table 1. (Continued.)

E_γ (keV)	$I^{(a)}_{\gamma+IC}$	E_i (keV)	E_f (keV)
489.2 ± 0.5	0.24 ± 0.05	708.3	218.9
504.0 ± 0.7	1.89 ± 0.54	902.3	398.5
519.5 ± 0.5	2.01 ± 0.15	682.5	162.8
541.1 ± 0.5	0.50 ± 0.15	939.5	398.5
545.3 ± 0.3	1.08 ± 0.07	708.3	162.8
546.7 ± 0.5	0.53 ± 0.08	939.5	392.8
559.7 ± 0.4	3.01 ± 0.12	722.3	162.8
575.8 ± 0.4	7.29 ± 0.84	575.9	0
576.9 ± 0.4	39.91 ± 1.51	577.0	0
579.0 ± 0.5		1154.5	575.9
583.3 ± 0.5	0.81 ± 1.59	708.3	124.4
590.6 ± 0.5	2.45 ± 0.83	1386.4	796.1
592.5 ± 0.4	0.41 ± 0.61	902.3	310.0
610.4 ± 0.4	0.38 ± 0.07	939.5	328.6
617.9 ± 0.3	1.47 ± 0.30	1772.3	1154.5
629.8 ± 0.5	0.85 ± 0.05	1027.9	398.5
631.3 ± 0.5	2.10 ± 0.51	755.7	124.4
633.5 ± 0.5	2.84 ± 0.09	796.1	162.8
635.2 ± 0.5	3.97 ± 0.27	1027.9	392.8
648.8 ± 0.5	1.03 ± 0.07	1027.9	379.3
671.7 ± 0.5	0.79 ± 0.21	796.1	124.4
682.5 ± 0.5	2.00 ± 0.13	682.5	0
699.5 ± 0.5	1.47 ± 0.06	1027.9	328.6
708.0 ± 0.3	1.29 ± 0.08	708.3	0
722.3 ± 0.4	0.46 ± 0.07	722.3	0
739.2 ± 0.3	1.12 ± 0.09	1154.5	415.2
755.5 ± 0.4	7.31 ± 0.47	755.7	0
774.5 ± 0.8	0.50 ± 0.10	1173.3	398.5
777.5 ± 0.5	2.36 ± 0.23	902.3	124.4
795.7 ± 0.5	0.89 ± 0.07	796.1	0
801.7 ± 0.5	0.74 ± 0.10	1704.	902.3
810.1 ± 0.2	1.64 ± 0.09	1386.4	575.9
815.1 ± 0.2	1.52 ± 0.11	939.5	124.4
840.3 ± 0.5	1.97 ± 0.32	1386.4	545.7
844.5 ± 0.5	1.01 ± 0.19	1154.5	310.0
844.5 ± 0.5	0.66 ± 0.16	1173.3	328.6
865.3 ± 0.5	0.56 ± 0.13	1027.9	162.8
869.9 ± 0.5	0.93 ± 0.24	1772.3	902.3
$895.4^{(b)} \pm 0.5$		1027.9	131.8
901.9 ± 0.5	4.68 ± 0.48	902.3	0
908.0 ± 0.7	1.16 ± 0.24	1704.	796.1
939.2 ± 0.3	3.92 ± 0.13	939.5	0
954.6 ± 0.5	0.93 ± 0.16	1173.3	218.9
976.6 ± 0.5	4.38 ± 0.16	1772.3	796.1
991.2 ± 0.5	0.25 ± 0.07	1154.5	162.8
994.3 ± 0.5	0.69 ± 0.05	1323.0	328.6
1027.7 ± 0.5	0.87 ± 0.67	1027.9	0
1029.0 ± 0.2	1.29 ± 0.67	1605.0	575.9
1039.5 ± 0.3	1.93 ± 0.14	1835.7	796.1
1049.9 ± 0.6	3.61 ± 0.25	1772.3	722.3
1058.0 ± 0.5	1.93 ± 0.24	1386.4	328.6
1076.0 ± 0.5	0.63 ± 0.12	1386.4	310.0
1160.1 ± 0.5	0.82 ± 0.13	1323.0	162.8
1167.1 ± 0.5	0.13 ± 0.06	1386.4	218.9
1222.4 ± 0.7	0.48 ± 0.03	1799.6	577.0
1373.3 ± 0.5	1.53 ± 0.07	1772.3	398.5
1386.0 ± 0.4	1.06 ± 0.05	1386.4	0

Table 1. (Continued.)

E_γ (keV)	$I^{(a)}_{\gamma+IC}$	E_i (keV)	E_f (keV)
1392.6 ± 0.5	1.49 ± 0.17	1772.3	379.3
1441.9 ± 0.7	0.14 ± 0.01	1605.0	162.8
1457.0 ± 0.5	1.02 ± 0.08	1835.7	379.3
1481.3 ± 0.5	0.87 ± 0.03	1605.0	124.4
1541.0 ± 0.7	0.19 ± 0.03	1704.	162.8
1605.1 ± 0.6	0.92 ± 0.14	1605.0	0
1609.2 ± 0.6	2.15 ± 0.15	1772.3	162.8
1636.9 ± 0.5	0.63 ± 0.32	1799.6	162.8
1648.0 ± 0.7	2.52 ± 0.10	1772.3	124.4
1672.7 ± 0.4	0.24 ± 0.07	1835.7	162.8
1675.0 ± 0.6	0.89 ± 0.06	1799.6	124.4
1711.2 ± 0.3	1.57 ± 0.05	1835.7	124.4
1771.9 ± 0.6	0.32 ± 0.03	1772.3	0
1799.6 ± 0.6	0.25 ± 0.02	1799.6	0
1835.8 ± 0.6	0.14 ± 0.01	1835.7	0
1943.5 ± 0.7	0.39 ± 0.07	1943.5	0
1950.0 ± 0.7	0.26 ± 0.05	1950.0	0
1988.4 ± 1.0	0.16 ± 0.03	1988.4	0
3304.8 ± 1.0	0.98 ± 0.13	3304.8	0

(a) For the absolute intensity per 100 decays multiply by 0.1533(24).
(b) Placement based in energetics.

The lines observed in previous β-decay studies [7,8, 17] are confirmed in this work except for the 438(2) keV line seen in ref. [7] that is not present in our spectra (see fig. 2).

The line at 576 keV reported in previous work [7,8] has been fitted as a doublet. The analysis of this γ-ray shows a low-energy tail. In addition the width of the peak is 20% larger than the average for γ-lines in the region. By fixing the width of the line to the standard value in the region it is possible to fit the peak within two Gaussian distributions centered at 575.8 and 576.9 keV with an intensity ratio of one to four (see table 1). Similarly, a doublet at 266 keV could now be resolved into two γ-transitions at 265.7 and 267.0 keV, respectively. Due to the better resolution of the detector at low energy, both contributions were observable.

At the bottom station, β-gated γ singles and $\gamma\gamma$ coincidences were recorded to establish the decay scheme. Table 2 lists the observed coincidences. Some of the listed coincident transitions, marked with an asterisk in the table, could not be placed in the decay scheme because the criterion used to build the level scheme was not satisfied (see subsect. 3.3). In most cases they also did not satisfy the symmetry of the coincidence matrix.

The 101.3 keV line clearly observed in the upper station is not seen in coincidence with any other γ-line. Its temporal behaviour also differs from the other γ-lines assigned to the decay. See, for instance, the difference in relative intensity of the 101.3 keV and the 124.4 keV lines between the spectra obtained at the bottom (fig. 1) and the upper (inset of fig. 1) stations. Already observed in the previous β-decay study by Davids *et al.* [18], this line was demonstrated by Garcia Bermudez *et al.* [10]

Table 2. Gamma-lines in coincidence with transitions belonging to ^{72}Br. The peaks marked with an asterisk are not placed in the decay scheme.

E (keV) gate	E_γ(keV) coincidence
30.5	178.5, 283.4
38.8	124.4
87.2	91.5, 196.2, 489.2 706*, 954.6, 1167.1
105.3	147.2, 162.7, 178.5, 208.9, 309.9
117.8	196.2
124.4	38.8, 147.2, 177.2, 178.5*, 183.3, 185.5, 186.8*, 204.4, 230.1, 252.4, 254.9, 274.2, 290.7, 414.5, 452.3, 484.7, 583.3, 631.3, 671.9, 777.5, 815.1, 869.9, 976.6, 1039.5, 1049.9, 1277.6*, 1373.3, 1392.6, 1481.3, 1552.6*, 1648.0, 1675.0, 1711.2
147.2+146.2	124.4, 160.8, 162.7, 265.7, 363.1*, 415.1
162.7	85.9*, 147.2, 183.3, 230.1, 252.4, 414.5, 519.2, 545.3, 559.7, 590.6, 592.5, 633.5, 739.2, 762.7*, 865.3, 908.0, 976.6, 991.2, 1039.5, 1049.9, 1160.1, 1441.9, 1541.0, 1609.2, 1636.9, 1672.7
177.2	124.4, 132.5, 274.2, 398.4, 579.0, 810.1, 1029.0
178.5	105.3, 235.5, 265.7, 485.9, 592.5, 976.6, 1029.0, 1076.0, 1154.8*, 1321.2*, 1561.0*
196.2	87.2, 313.8, 380.8, 445.7*, 597.1*, 665.0*, 908.0
230.1	162.7, 183.3
235.5	162.7, 178.5, 309.9, 356.3, 482.5, 840.3
252.4	124.4, 162.7, 257.8*, 1485.0*
254.9	124.4
265.7	147.2, 178.5, 208.9, 309.9, 451.4, 810.1, 1029.0
283.4	226.5*, 1018*
309.9	88.5, 105.3, 233.9*, 235.5, 265.7, 412.1, 484.7, 485.9, 590.6, 592.5, 617.9, 810.1, 844.5, 869.9, 976.6, 1029.0, 1049.9, 1076.0, 1725*(+^{72}Br), 2235*
313.8	196.2
328.4	379.3, 610.4, 699.5, 844.5, 994.3, 1058.0, 1103.0*, 1312*
379.3	130.5, 328.4, 862.03 (^{72}Br), 1227.3 (^{72}Br), 1392.6, 1457.0
380.8	415.1, 576*, 590.6, 908.0, 976.6, 1039.5
392.7	183.3, 546.7, 635.2, 1161.7*
398.4	147.2, 177.2, 504.0, 579.0, 629.8, 774.5, 810.1, 1029.0, 1373.3

Table 2. (Continued.)

E (keV) gate	E_γ(keV) coincidence
412.1	178.5, 309.9, 322.0*, 1049.9
414.5	162.7
415.1	160.8, 307.0, 380.8, 590.6, 739.2, 908.0, 976.6, 1039.5
451.4	265.7, 178.5, 309.9
452.3	124.4
482.5	235.5, 309.9
484.7	124.4, 309.9, 356.3, 398.4, 504.0, 592.5, 777.5, 901.9, 1319*, 1614*, 1725*
485.9	309.9, 590.6, 908.0, 976.6, 1039.5
617.9	309.9, 415.1, 739.2, 844.5
699.5	328.4
739.2	162.7, 309.9, 415.1
755.5	766*, 793*
844.5	309.9, 328.4, 413.0*, 617.9, 858*
901.9	484.7, 801.7 , 869.9
976.6	162.7, 309.9, 380.8, 415.1, 485.9, 633.5
994.3	328.4
1039.5	162.7, 178.5, 196.2, 218.8, 252.4, 309.9, 380.8, 415.1, 485.9, 633.5
1049.9	102.8*, 124.4, 146.2, 162.7, 307.0, 309.9, 412.1, 415.1, 559.7
1373.3	88.5, 309.9, 398.4
1711.2	124.4

to correspond to the decay of an isomeric state in ^{72}Br at 101.3 keV excitation energy with a measured $T_{1/2}$ of 10.3(6) s. The intensity given for this line in table 1 is corrected for the difference in $T_{1/2}$ of the 101.3 level [10]. Taking into account the decay laws and the integrated time interval, the reported intensity has been multiplied by a factor of 0.96(4).

A new $T_{1/2}$ value for ^{72}Kr was inferred by the study of the temporal behaviour of the γ intensities obtained in the multispectrum mode. Independent values of the half-life were obtained from the most intense γ-lines: 124.4, 162.7, 252.4, 309.9, 415.1 and 575.8 + 576.9 keV. The weighted average from the six values yields $T_{1/2} = 17.1 \pm 0.2$ s. This value agrees with the previous results $T_{1/2} = 16.7 \pm 0.6$ s [7] and 17.4 ± 0.4 s [8], but a higher precision has been achieved. Figure 3 shows the decay curves of some strong γ-lines assigned to the ^{72}Kr decay and two intense γ-transitions from the ^{72}Br decay. The temporal behaviour of the 101.3 keV γ-ray is fitted with two components where one corresponds to the feeding of the 101.3 keV level from γ-transitions following the ^{72}Kr decay (17 s) and the other to the decay of this isomeric state (11 s).

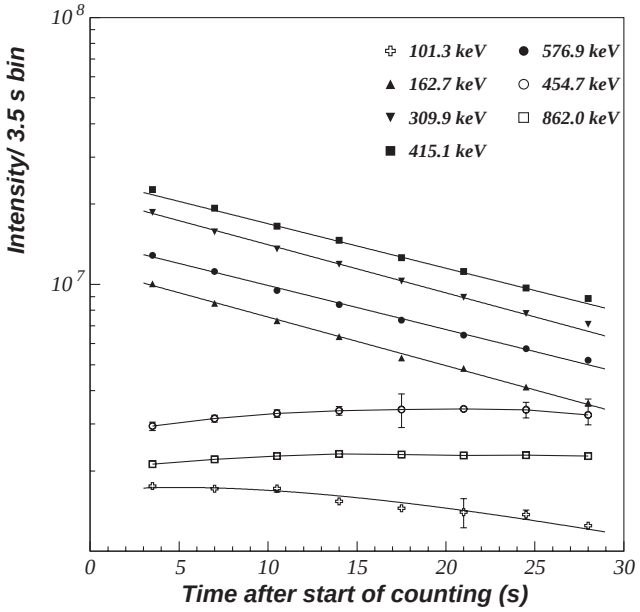

Fig. 3. Temporal behaviour of the intensity for different γ-lines following the ^{72}Kr decay (full symbols), the ^{72}Br decay (empty symbols) and the de-excitation of the isomeric 101.3 keV state in ^{72}Br (empty cross symbols).

3.2 Spin and parity of the ^{72}Br ground state

The previously reported ^{72}Br ground-state spin and parity assignment differ significantly. Data on the decay of ^{72}Kr [7,8] have been obtained in two independent experiments, using fusion-evaporation reactions as well as the He-jet technique. The resulting decay schemes are similar, but the beta branching ratios show large discrepancies, with the g.s. feeding varying from 54% in [7] to $9 \pm 15\%$ reported in [8] (or even as low as $2 \pm 11\%$ depending on the position of the 124.4 keV transition). The former value favours and the latter is compatible with a $J^\pi = 1^+$ assignment to the g.s. Later the only detailed study of the β-decay of ^{72}Br performed to date [9] suggests a 3^+ value for the J^π of the ^{72}Br (g.s.) on the basis of a 5.0(9)% beta-feeding ($\log f_0 t = 7.0$) to the 1636.86(13) keV state established as 4^+ [19,20]. The latter value has been retained in the compilations and used to characterize the g.s. of ^{72}Br.

A reliable estimate of the g.s. transition can be obtained from a quantitative comparison of the parent and the daughter activities. In our work gamma intensities were taken from our decay scheme for the ^{72}Kr activity and from Collins *et al.* [9] for the decay of the ^{72}Br daughter. The evaluation was based on the observation of four γ-lines in the ^{72}Kr decay (162.7, 309.9, 415.1 and 575.8 + 576.9 keV) and the four most intense gamma-lines in ^{72}Br decay (454.7, 862.0, 1136.9, 1316.7 keV). The intensity of the g.s. transition was obtained from the measurements at both the upper and lower counting stations under the conditions described earlier.

The weighted averaged values of the β-decay g.s. feeding determined in the two stations are consistent. At the

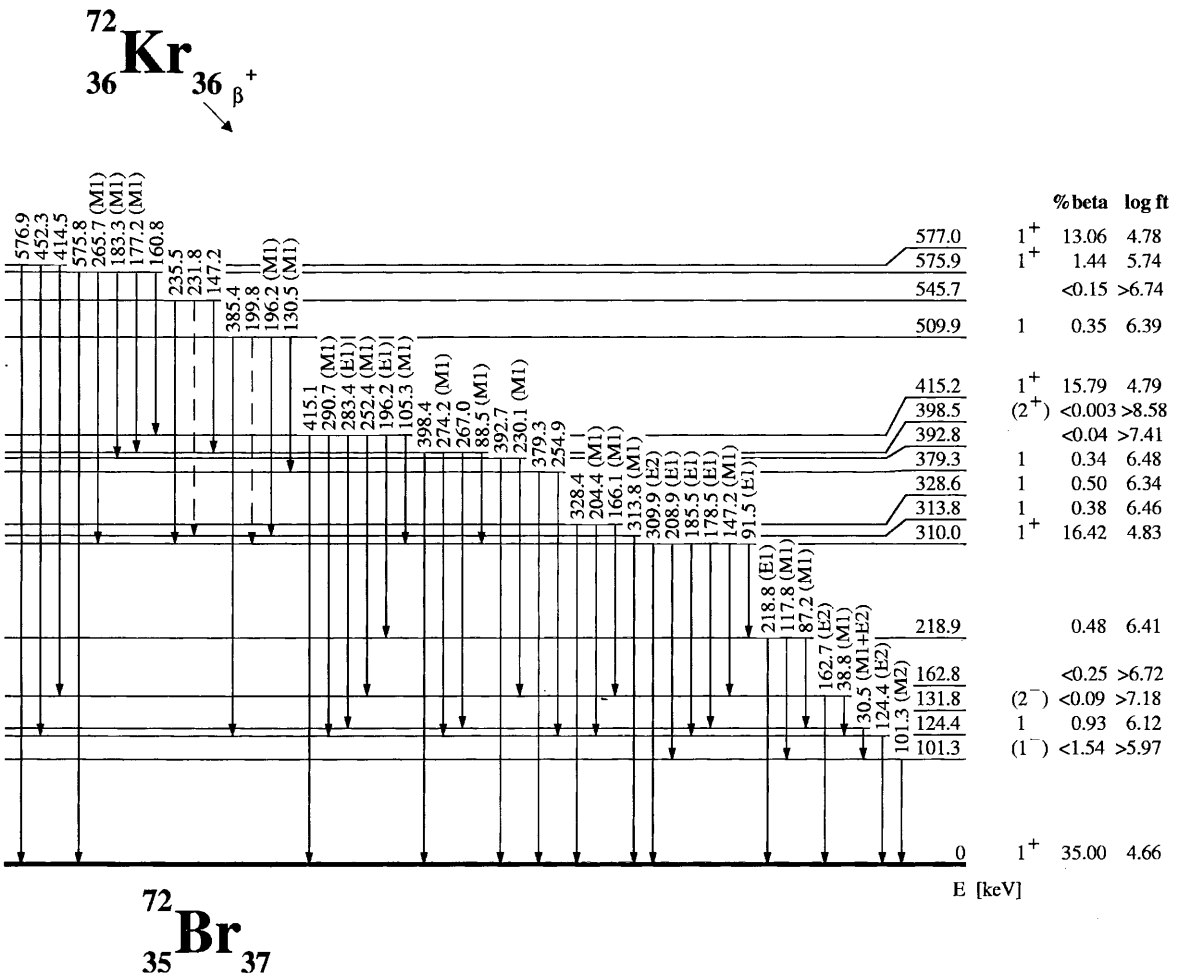

Fig. 4a. Low-energy part of the proposed decay scheme of ^{72}Kr. The transitions indicated by dashed lines are firmly established, but their intensities could not be obtained.

upper station no parasitic build-up of ^{72}Br activity can occur, so the value of $35 \pm 3\%$ deduced from this station has been chosen for the ground-state beta feeding. This value lies between previous β-decay results [7,8] but is much more accurate. By combining the uncertainties on the transitions to all levels in ^{72}Br, the total uncertainty in the β-feeding to the g.s. is reduced to 1%. The corresponding $\log f_0 t$ ($4.66^{+0.20}_{-0.18}$) unambiguously points to an allowed g.s. $\rightarrow$ g.s. transition thus fixing the spin and parity of the ^{72}Br to be 1^+. In the adopted ^{72}Br decay scheme [9] no g.s. feeding is considered. If such a feeding were not negligible, it would increase our value of the feeding of the ^{72}Br g.s. and therefore would not change the J^π assignment. One should mention here that the low value of the magnetic moment for ^{72}Br g.s. measured by Griffiths *et al.* [21] is not compatible with the existence of any low-lying 3^+ state in this nucleus.

Concerning the in-beam studies, it should be noted that none of the three bands identified in ^{72}Br [10–12] are clearly associated with a 3^+ ground state. Therefore the change of spin of the ^{72}Br ground state should have minor impact for the in-beam studies. To better understand the new J^+ value in terms of the wave function of the g.s. of ^{72}Br, we have considered possible wave functions in the frame of self-consistent deformed mean-field calculations with the SG2 Skyrme force and pairing correlations, see details of the calculation in [22]. The decay is of the type p $\rightarrow$ n, therefore the calculations favour neutron orbitals with occupation probability ≤ 0.5 in the even nucleus. For the even-even case one finds several possible deformed orbitals very close to the Fermi energy and therefore good candidates to allocate the odd particle. For prolate deformation the calculation gives a minimum for a deformation parameter $\beta = 0.14$ and two configurations compete. Both cases involve an odd proton and an odd neutron in the same orbital, leading to the configuration $\pi[301]3/2^- \otimes \nu[301]3/2^-$ with an occupation probability of ~ 0.5. The Gallager-Moszkowski rule [23] favours $J = 3^+$ ($T = 0$). Equally probable is the configuration $\pi[301]3/2^- \otimes \nu[303]5/2^-$ with occupation probability of 0.52 for the proton orbital and 0.22 for the neutron one. In this case, the same Gallager-Moszkowski rule [23] favours the antiparallel coupling $J = 1^+$ ($T = 0, 1$). For the oblate case and the same force a deformation $\beta = -0.25$ is obtained, with the most favoured configuration involving the neutron and the proton in the same

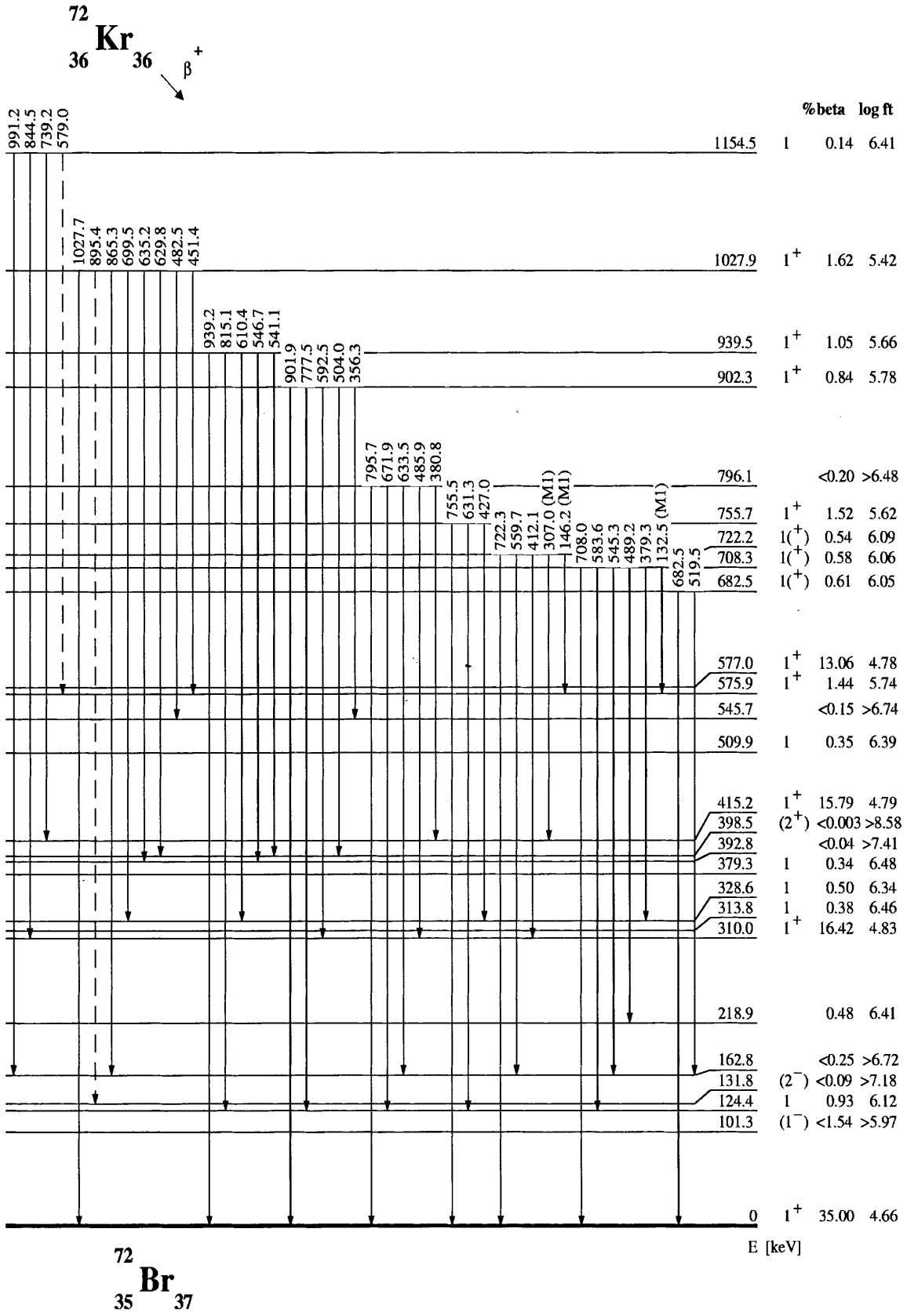

Fig. 4b. Middle part of the adopted decay scheme of ^{72}Kr. The transitions indicated by dashed lines are firmly established, but their intensities could not be obtained.

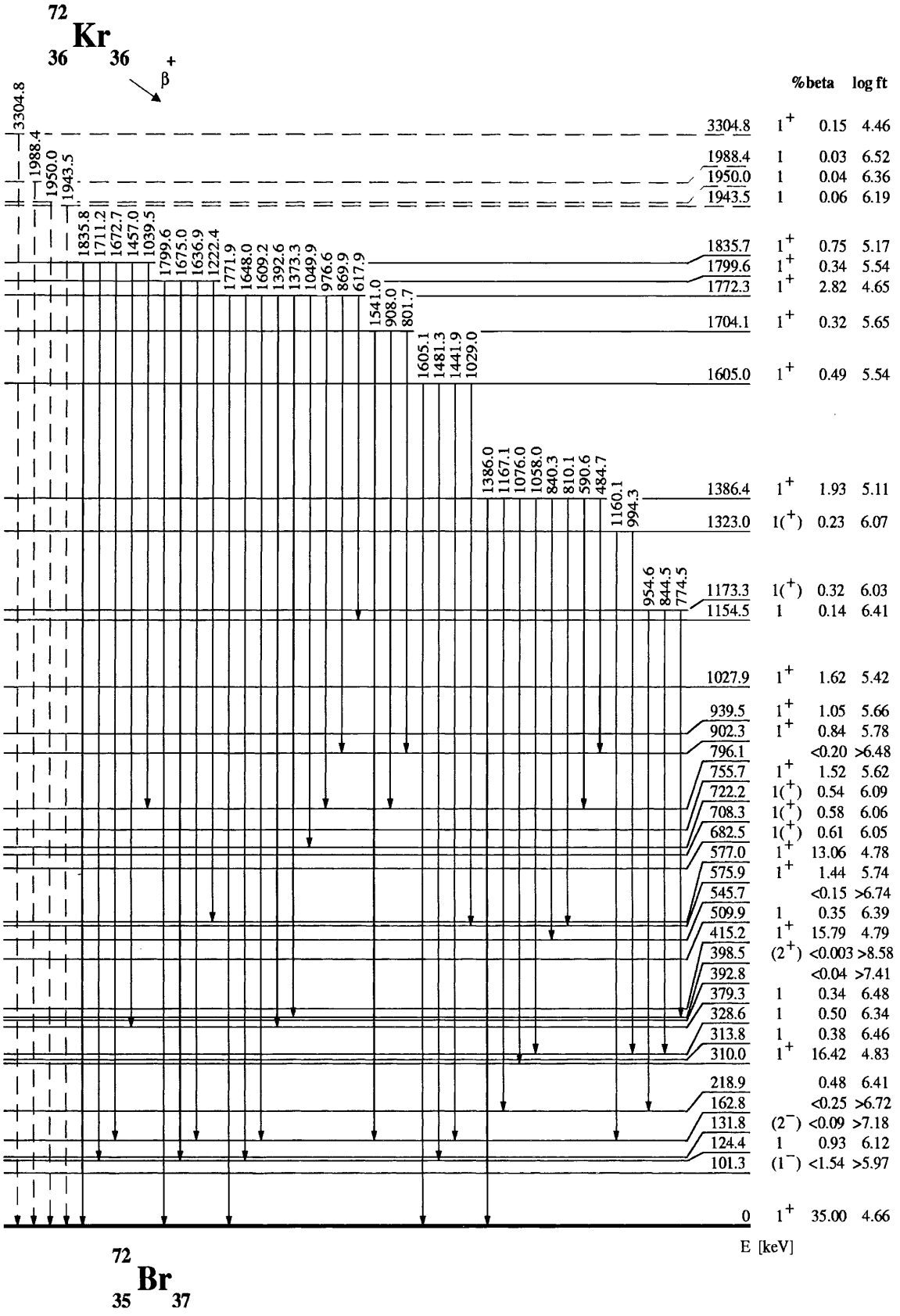

Fig. 4c. Upper part of the adopted decay scheme of ^{72}Kr. The levels indicated by dashed lines are not firmly established according to the criterion applied in this work (see text). The transitions indicated by dashed lines are chosen to connect these levels to the g.s. of ^{72}Br.

orbital, *i.e.* $\pi[404]9/2^- \otimes \nu[404]9/2^-$, and corresponding to $J = 9^+$ ($T = 0$). To calculate the magnetic moment corresponding to these three configurations we have assumed the validity of the asymptotic-quantum-number description and used the simple expression derived by Bohr and Mottelson [24] for deformed nuclei in the form given on page 1289 of ref. [23] (a more general formulation is given by Moya de Guerra [25]). One gets for $J = 1^+$, $\mu = 0.71\mu_N$; for $J = 3^+$, $\mu = 1.77\mu_N$ and for $J = 9^+$, $\mu = 4.8\mu_N$, to be compared to the magnetic moment of 0.55(21) μ_N measured by Griffiths *et al.* [21]. In summary, the strong beta-feeding to the ^{72}Br ground state favours $J = 1^+$, which in our calculations correspond to a prolate nucleus with a deformation parameter $\beta = 0.14$. The dominant odd-odd particle configuration in this case is $\pi[301]3/2^- \otimes \nu[303]5/2^-$, which implies a small value for the g.s. magnetic moment consistent with the experimental value of Griffiths *et al.* [21].

3.3 Decay scheme of ^{72}Kr

Figures 4a-4c show the decay scheme resulting from the analysis of our data together with the J^π assignments, the percentage of β-feeding and the log f_0t values. Twenty-seven new levels and 116 newly assigned transitions are reported, extending the knowledge of low-spin states in ^{72}Br up to 3.3 MeV excitation energy. The energy of the levels is calculated from the weighted mean of the different transitions feeding and de-exciting it. Table 3 presents the spin-parity assignments, de-exciting γ-transitions and γ-ray branching ratios of the levels. Table 4 lists the β-feeding, log f_0t and B(GT) values for the different levels in ^{72}Br fed in this work. The position of each new level has been determined on the basis of the criterion that the level is connected by at least two transitions to previously established levels with the exception of the highest energy levels at 1943.5, 1950.0, 1988.4 and 3304.8 keV which are shown in fig. 4c with dashed lines. These levels have been established on the basis of a single high-energy γ-line to the g.s. which follows the temporal behaviour of the ^{72}Kr decay.

In the newly established level scheme (figs. 4a-4c) all the levels reported previously with spin less than four [7,8, 10–12] are found except for the level at 230 keV. However, there are some differences in the assignments of position and multipolarity of the transitions that will be discussed below. A brief description of the more complicated level assignment is also outlined.

In the case of the 101.3 keV isomeric level, the connecting transitions to other levels are proposed on the basis of the energy differences between the transition to the g.s. and to the isomeric state, except for the 131.8 keV, $J^\pi = 2^-$ state which does not decay to the g.s. As proposed by Garcia Bermudez *et al.* [10], the position of the 101.3 keV level is kept as the first excited level in ^{72}Br. The $M2$ character of the 101.3 keV transition has been established in ref. [10] on the basis of intensity balance arguments. The conversion coefficient of the 101.3 keV γ-ray was measured by Griffiths *et al.* [21] to be $\alpha_K = 1.4(3)$, which assigned this transition as a pure $M2$. An $M2$ character for this

Table 3. Excitation energies, spins, parities, de-exciting γ-transitions and γ-ray branching ratios of adopted levels in ^{72}Br.

E_x (keV)	J^π	E_γ (keV)	$I_{\gamma+\mathrm{IC}}$ (%)
101.3 ± 0.3	(1^-)	101.3	100
124.4 ± 0.2	1	124.4	100
131.8 ± 0.6	(2^-)	30.5	100
162.8 ± 0.3		38.8	4.2 ± 1.0
		162.7	95.8 ± 1.0
218.9 ± 0.3		87.2	86.8 ± 2.8
		117.8	7.8 ± 1.9
		218.8	5.4 ± 2.0
310.0 ± 0.1	1^+	91.5	0.3 ± 0.1
		147.2	2.8 ± 0.3
		178.5	13.1 ± 1.0
		185.5	0.1 ± 0.1
		208.9	3.4 ± 0.3
		309.9	80.3 ± 1.0
313.8 ± 0.3	1	313.8	100
328.6 ± 0.2	1	166.1	8.0 ± 1.4
		204.4	7.3 ± 1.2
		328.4	84.6 ± 1.7
379.3 ± 0.4	1	254.9	19.0 ± 3.1
		379.3	81.0 ± 3.1
392.8 ± 0.2		230.1	38.8 ± 2.0
		392.7	61.2 ± 2.0
398.5 ± 0.1	(2^+)	88.5	9.5 ± 7.4
		267.0	9.3 ± 2.3
		274.2	20.4 ± 2.0
		398.4	60.8 ± 5.3
415.2 ± 0.1	1^+	105.3	3.1 ± 0.3
		196.2	2.1 ± 0.7
		252.4	14.1 ± 0.7
		283.4	4.4 ± 0.2
		290.7	0.3 ± 0.1
		415.1	76.0 ± 1.2
509.9 ± 0.3	1	130.5	32.1 ± 8.6
		196.2	48.6 ± 12.7
		385.4	19.3 ± 5.2
545.7 ± 0.1		147.2	15.6 ± 5.2
		235.5	84.4 ± 5.2
575.9 ± 0.1	1^+	160.8	5.1 ± 0.6
		177.2	6.4 ± 0.7
		183.3	13.1 ± 1.6
		265.7	22.3 ± 1.6
		575.8	53.1 ± 3.0
577.0 ± 0.2	1^+	414.5	48.0 ± 2.5
		452.3	5.4 ± 0.3
		576.9	46.6 ± 2.3
682.5 ± 0.3	$1^{(+)}$	519.5	50.1 ± 2.4
		682.5	49.9 ± 2.4
708.3 ± 0.1	$1^{(+)}$	132.5	6.1 ± 2.8
		379.3	3.4 ± 1.6
		489.2	6.2 ± 2.9
		545.3	28.6 ± 12.1
		583.3	21.5 ± 33.0
		708.0	34.1 ± 14.4
722.2 ± 0.1	$1^{(+)}$	146.2	2.0 ± 1.4
		307.0	16.2 ± 1.4
		412.1	33.0 ± 1.2
		559.7	42.3 ± 1.5
		722.3	6.5 ± 1.0

Table 3. (Continued.)

E_x (keV)	J^π	E_γ (keV)	$I_{\gamma+\mathrm{IC}}$ (%)
755.7 ± 0.2	1^+	427.1	4.9 ± 0.6
		631.3	21.2 ± 4.2
		755.5	73.9 ± 4.0
796.1 ± 0.1		380.8	34.5 ± 1.2
		485.9	25.2± 0.8
		633.5	25.3± 0.8
		671.7	7.0± 1.7
		795.7	8.0± 0.6
902.3 ± 0.1	1^+	356.3	5.6 ± 0.7
		504.0	19.1± 4.7
		592.5	4.1± 5.9
		777.5	23.8± 2.9
		901.9	47.3± 4.8
939.5 ± 0.1	1^+	541.1	7.3 ± 2.1
		546.7	7.8± 1.2
		610.4	5.5± 1.0
		815.1	22.2± 1.4
		939.2	57.2± 2.0
1027.9 ± 0.1	1^+	451.4	9.7 ± 1.8
		482.5	7.8± 1.9
		629.8	8.1± 0.8
		635.2	37.5± 3.1
		648.8	9.7± 0.9
		699.5	13.9± 1.2
		865.3	5.2± 1.3
		1027.7	8.2± 5.8
1154.5 ± 0.1	1	739.2	47.0 ± 4.5
		844.5	42.7± 5.0
		991.2	10.3± 2.7
1173.3 ± 0.2	$1^{(+)}$	774.5	23.9 ± 4.5
		844.5	31.5± 5.9
		954.6	44.6± 5.8
1323.0 ± 0.3	$1^{(+)}$	994.3	45.9 ± 4.2
		1160.1	54.1± 4.2
1386.4 ± 0.1	1^+	484.7	21.9 ± 2.1
		590.6	19.5± 5.4
		810.1	13.0± 1.2
		840.3	15.7± 2.4
		1058.0	15.4± 2.0
		1076.0	5.0± 1.0
		1167.1	1.0± 0.5
		1386.0	8.4± 0.7
1605.0 ± 0.1	1^+	1029.0	39.9 ± 12.5
		1441.9	4.5± 1.0
		1481.3	27.0± 5.7
		1605.1	28.6± 6.7
1704.1 ± 0.1	1^+	801.7	35.4 ± 5.1
		908.0	55.6± 5.8
		1541.0	9.0± 1.9
1772.3 ± 0.1	1^+	617.9	8.0 ± 1.5
		869.9	5.1± 1.2
		976.6	23.8± 1.0
		1049.9	19.6± 1.2
		1373.3	8.3± 0.4
		1392.6	8.1± 0.9
		1609.2	11.7± 0.8
		1648.0	13.7± 0.6
		1771.9	1.7± 0.2

Table 3. (Continued.)

E_x (keV)	J^π	E_γ (keV)	$I_{\gamma+\mathrm{IC}}$ (%)
1799.6 ± 0.2	1^+	1222.4	21.4 ± 3.3
		1636.9	27.8 ± 10.2
		1675.0	39.5± 5.8
		1799.6	11.3± 1.9
1835.7 ± 0.1	1^+	1039.5	39.4 ± 1.9
		1457.0	20.8± 1.4
		1672.7	5.0± 1.3
		1711.2	32.0± 1.3
		1835.8	2.8± 0.3
1943.5 ± 0.7	1	1943.5	100
1950.0 ± 0.7	1	1950.0	100
1988.4 ± 1.0	1	1988.4	100
3304.8 ± 1.0	1^+	3304.8	100

Table 4. Beta branching ratios, $\log f_0 t$ and B(GT) values for the ^{72}Br levels.

E (keV)	$\%\beta$	$\log f_0 t$	B(GT) 10^{-5}
0.0	35.00 ± 1.03	$4.66^{+0.18}_{-0.20}$	8523 ± 830
101.3 ± 0.3	< 1.53	> 5.97	< 419
124.4 ± 0.2	0.93 ± 0.44	$6.17^{+0.21}_{-0.32}$	261 ± 135
131.8 ± 0.6	< 0.09	> 7.18	< 25
162.8 ± 0.3	< 0.252	> 6.72	< 74
218.9 ± 0.3	0.48 ± 0.19	$6.41^{+0.18}_{-0.25}$	150 ± 66
310.0 ± 0.1	16.42 ± 0.65	$4.83^{+0.06}_{-0.06}$	5737 ± 747
313.8 ± 0.3	0.385 ± 0.086	$6.46^{+0.13}_{-0.15}$	135 ± 40
328.6 ± 0.2	0.499 ± 0.066	$6.34^{+0.10}_{-0.10}$	178 ± 38
379.3 ± 0.4	0.34 ± 0.15	$6.48^{+0.20}_{-0.31}$	128 ± 65
392.8 ± 0.2	< 0.039	> 7.41	< 15
398.5 ± 0.1	< 0.003	> 8.58	< 1
415.2 ± 0.1	15.79 ± 0.71	$4.79^{+0.06}_{-0.06}$	6278 ± 863
509.9 ± 0.3	0.351 ± 0.087	$6.39^{+0.14}_{-0.17}$	157 ± 50
545.7 ± 0.1	< 0.15	> 6.74	< 71
575.9 ± 0.1	1.44 ± 0.18	$5.74^{+0.09}_{-0.10}$	702 ± 147
577.0 ± 0.2	13.06 ± 0.65	$4.78^{+0.07}_{-0.07}$	6371 ± 925
682.5 ± 0.3	0.614 ± 0.035	$6.05^{+0.07}_{-0.07}$	344 ± 53
708.3 ± 0.1	0.580 ± 0.032	$6.06^{+0.07}_{-0.07}$	336 ± 52
722.2 ± 0.1	0.537 ± 0.053	$6.09^{+0.09}_{-0.09}$	317 ± 61
755.7 ± 0.2	1.52 ± 0.11	$5.62^{+0.08}_{-0.08}$	936 ± 161
796.1 ± 0.1	0.20 ± 0.14	$6.48^{+0.28}_{-0.60}$	130 ± 97
902.3 ± 0.1	0.84 ± 0.16	$5.79^{+0.12}_{-0.14}$	635 ± 176
939.5 ± 0.1	1.050 ± 0.051	$5.67^{+0.07}_{-0.07}$	838 ± 129
1027.9 ± 0.1	1.62 ± 0.13	$5.42^{+0.08}_{-0.09}$	1471 ± 269
1154.5 ± 0.1	0.139 ± 0.057	$6.41^{+0.20}_{-0.28}$	152 ± 73
1173.3 ± 0.2	0.321 ± 0.039	$6.03^{+0.10}_{-0.11}$	361 ± 81
1323.0 ± 0.3	0.241 ± 0.022	$6.07^{+0.09}_{-0.10}$	329 ± 67
1386.4 ± 0.1	1.93 ± 0.16	$5.11^{+0.09}_{-0.09}$	3031 ± 591
1605.0 ± 0.1	0.49 ± 0.11	$5.54^{+0.14}_{-0.17}$	1124 ± 355
1704.1 ± 0.1	0.321 ± 0.041	$5.65^{+0.11}_{-0.12}$	870 ± 214
1772.3 ± 0.1	2.82 ± 0.12	$4.65^{+0.08}_{-0.08}$	8655 ± 1529
1799.6 ± 0.2	0.344 ± 0.051	$5.54^{+0.12}_{-0.13}$	1112 ± 296
1835.7 ± 0.1	0.752 ± 0.036	$5.17^{+0.09}_{-0.09}$	2596 ± 477
1943.5 ± 0.7	0.059 ± 0.011	$6.19^{+0.14}_{-0.16}$	250 ± 76
1950.0 ± 0.7	0.040 ± 0.007	$6.36^{+0.14}_{-0.16}$	170 ± 51
1988.4 ± 1.0	0.025 ± 0.005	$6.52^{+0.14}_{-0.16}$	117 ± 37
3304.8 ± 1.0	0.151 ± 0.02	$4.46^{+0.13}_{-0.13}$	13508 ± 3571

transition is still compatible with our new spin and parity assignment, $J^\pi = 1^+$ for the ^{72}Br g.s. and the previously assigned $J^\pi = (1^-)$ for the level at 101.3 keV.

We confirm the level at 124.4 keV excitation energy placed by Garcia Bermudez *et al.* [10] on the basis of the many transitions observed in coincidence with the 124.4 keV line (see fig. 5). This line had already been observed in previous β-decay works [7,8], but it could not be placed in the level scheme because no $\gamma\gamma$ coincidences were observed. From the Q_β distribution measured in coincidence with the 124.4 keV γ-line, Schmeing *et al.* [7] suggested placing this transition at high excitation energy. In our scheme this level is dominantly fed by γ-transitions de-exciting higher levels, resulting in a very reduced direct β-feeding and in an apparent Q_β smaller than expected from the position of the level. The spin of this level was suggested to be 2 or 3 [10]. The 0.9(4)% β-feeding obtained in our work for the 124.4 keV level favours a $J = 1$ spin assignment ($\log f_1 t = 7.79(44)$).

The 131.8 keV level is well established by four transitions feeding it from above. The de-excitation proceeds via a single 30.5 keV transition measured to be of $M1$ character [10]. In order to satisfy the γ-intensity balance, an internal conversion coefficient of 20.7 had to be assumed, which corresponds to a 27% $E2$ admixture in this transition. Our $\log f_0 t$ lower limit of 7.2 is compatible with the previous $J^\pi = 2^-$ assignment [10].

The $J^\pi = 1^+$ assignment for the 162.8 keV level resulted from the previously established decay scheme of ref. [8] where a 10% feeding was determined from the γ-intensity balance of the 252.4 keV γ-ray feeding the state and the 162.7 keV transition de-exciting it. Our $\gamma\gamma$ coincidence study showed sixteen transitions feeding this state. An upper limit for the β-feeding of 0.25% has been obtained for a $M1$ 38.8 keV γ-ray and an $E2$ 162.7 keV ray de-exciting the level. If one increases the conversion coefficient of the 38.8 keV line to reflect a higher multipolarity, the γ-intensity balance for the 124.4 keV level is unphysical. The resulting $\log f_0 t$ lower limit of 6.72 excludes the $J^\pi = 1^+$ assignment of ref. [8].

A β^+ branching of 0.48(19)% for the 218.9 keV state results from our decay scheme. This level has previously been tentatively assigned as $J^\pi = 3^-$ [10]. Its γ-feeding from higher 1^+ states, *i.e.* the 310.0 and 415.2 keV levels, would then proceed through low-energy $M2$ transitions. These slower transitions would give a significant $T_{1/2}$ for the 310.0 and 415.2 levels, but this supposition is not compatible with the observed prompt coincidences between the transitions feeding and de-exciting these levels. The β-feeding yields a $\log f_1 t$ value of $8.01^{+0.40}_{-0.49}$ close to the limit of a first forbidden unique transition ($\Delta J = 2$, $\Delta\pi =$ yes). Being aware that our study could miss the placement of γ-lines feeding this level, which could reduce the β-feeding considerably, our result favours a maximum spin of $J = 2$ for this level. For $J^\pi = 1^-$, 2^-, the feeding from the 1^+ states would be via $E1$ transitions compatible with our observed coincidence data.

The level at 230 keV quoted by Garcia Bermudez *et al.* [10] and determined by energetics is not present in our decay scheme. In our work we observe a line at 230.1 keV in coincidence with the 162.7 keV γ-ray as clearly illustrated in fig. 6. This line connects the 162.8 keV level with the newly reported level at 392.8 keV.

The level at 310.0 keV is well established by six de-exciting transitions and nine feeding γ-lines. Among the latter we find a line at 235.5 keV, as shown in the bottom part of fig. 6, previously assigned on the basis of matching energies [10] to connect the 398.5 and the 162.8 keV levels. The 310.0 keV state is confirmed as 1^+ with a $\log f_0 t$ value of $4.83^{+0.06}_{-0.06}$ making it the lowest 1^+ excited state.

In this work a level at 313.8 keV has been determined on the basis of the coincidences observed between a γ-line of this energy and one of 196.2 keV. For the latter, the coincidence data shows two components, where the main one connects the established states at 218.9 and 415.2 keV. However, placing the 313.8 keV γ-ray above the 415.2 keV state, one should have seen the 415.1 keV line in the projection of the 313.8 keV gate as it is one of the most intense lines in the spectrum. As this is not the case we are confident of the composite character of the 196.2 keV line and in the assignment of a new level at 313.8 keV excitation energy for which a $J = 1$ spin is deduced based on the $\log f_0 t$ value of $6.46^{+0.13}_{-0.15}$.

The 379.3 keV level located in previous in-beam studies [10,11] has also been corroborated by our analysis, but the γ-peak of this energy seems to have several components. From the total intensity, we have subtracted the contribution of the 379.5 keV line belonging to the daughter decay by using the relative intensities of ref. [17]. We have established a level at 328.6 keV based on the matching of three pairs of coincidence, *i.e.* the 124.4 keV line with the 204.4 keV line, the 162.7 keV line with the 166.1 keV line and the 328.4 keV line connecting this state to the g.s. The gate at 328.4 keV γ-ray reveals a strong coincidence with a 379.3 keV line connecting this level to the 708.3 keV state established by five transitions to other low-lying states. To extract the intensity of the two components we have used the relative branching ratios measured in the in-beam work [11] for the 379.3 keV level. A β-feeding of 0.34(15)% to the 379.3 keV level yields a $\log f_0 t$ of $6.48^{+0.20}_{-0.31}$ compatible only with $\Delta J = 0, 1$.

The 415.1 keV transition, which is the most intense γ-ray following the decay of ^{72}Kr, was also observed to have a composite character. The analysis of the $\gamma\gamma$ coincidences revealed that the projection of gates placed at the left and right sides of the 415.1 keV peak gave different lines in coincidence (see table 2). The existence of a level at 415.2 keV excitation energy was confirmed as established in previous works [7,8]. In spite of the composite character of this γ-line which affects the deduced beta-feeding for the 415.2 keV level we agree that it is still strongly beta fed in the beta-decay and it has therefore been definitively assigned as a 1^+ state. The second gamma-transition, with an energy assigned from the coincidence data of 414.5 keV, feeds the 162.8 keV level.

Concerning the previously reported [7,8] state at 576 keV, we find that the 576 keV peak is 20% broader than the rest of the γ-lines in the same region, as already

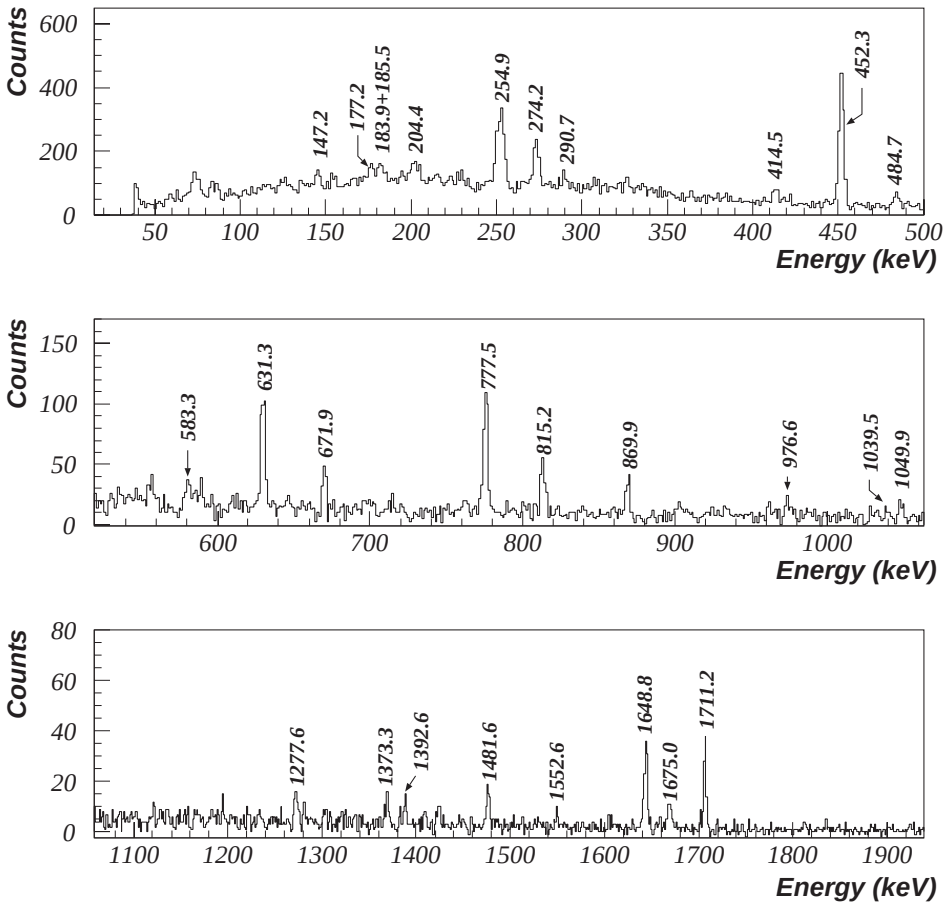

Fig. 5. The gamma-ray spectrum of the 80% efficiency HPGe detector at the collection point (bottom station) gated with the 124.4 keV transition observed in the 70% HPGe detector. The "true" coincidence nature of the labelled peaks was verified using reciprocal gating.

mentioned in subsect. 3.1. The 577.0 keV level is fixed by the 452.3 keV transition seen in the gate on the 124.4 keV peak and the 576.9 keV γ-ray itself. The position of the component at 575.8 keV is well determined by five transitions out of this level at 575.9 keV and four that populate it (see fig. 4b). The $\log f_0 t$ obtained for these two levels favours a spin-parity assignment for both levels of 1^+.

Strong coincidences are observed between the 844.5 keV transition and the 309.9 keV and 328.4 keV γ-rays. A search for a 18.5 keV transition that would connect the two states with those same energies was performed in the spectrum recorded with the low-energy γ-ray detector. This detector, placed at the upper station, was sensitive down to 8 keV. The non-observation of such a line establishes an upper level of 0.02% for its relative intensity. Possible multipolarities for this 18.5 keV transition compatible with the spin of the two connecting states are $E1$ ($\alpha = 10.9$), $M1$ ($\alpha = 15.0$) and $E2$ ($\alpha = 392.2$). If the transition were mainly $E2$ the most intense lines in coincidence with the 328.4 keV γ-ray, namely 379.3, 610.4, 699.5 and 1058.0 keV, should have been seen in the gate of the 309.9 keV γ-line, but this was not the case. If the multipolarity were $E1$ or $M1$ ($I_{\gamma+\mathrm{IC}} \leq 0.33\%$) the intensity of the 309.9 keV line in coincidence with the 844.5 keV γ-ray should have been 5% of the intensity of the 328 keV in the same projection. As the intensity of the 309.9 keV is higher than the 328.4 keV γ-ray in the gate of the 844.5 keV line we are confident that no connection exists between these two states. Therefore, we assign two transitions of ~ 844.5 keV to feed both levels independently, connecting them to the already well-established states at 1154.5 and 1173.3 keV (see table 3 and fig. 4b). The relative intensities of the two components have been extracted from the coincidence data.

The new levels presented in this work extend up to 3.3 MeV excitation energy. Most of them are characterized by allowed β-transitions yielding unambiguous 1^+ assignments (see the decay scheme shown in figs. 4a-4c). A large gap between 2.0 and 3.3 MeV excitation energy is observed. From the $\gamma\gamma$ data (table 2) there are indications of coincidences with high-energy γ-lines which could originate from levels located between 2 and 3 MeV excitation energy. However in these cases the criterion used to build the level scheme was not satisfied.

The levels represented with a dashed line in fig. 4c have been assigned to ^{72}Br on the basis of a high-energy gamma line with the correct $T_{1/2}$ and subsequently placed as feeding the g.s. The resulting excitation energies for

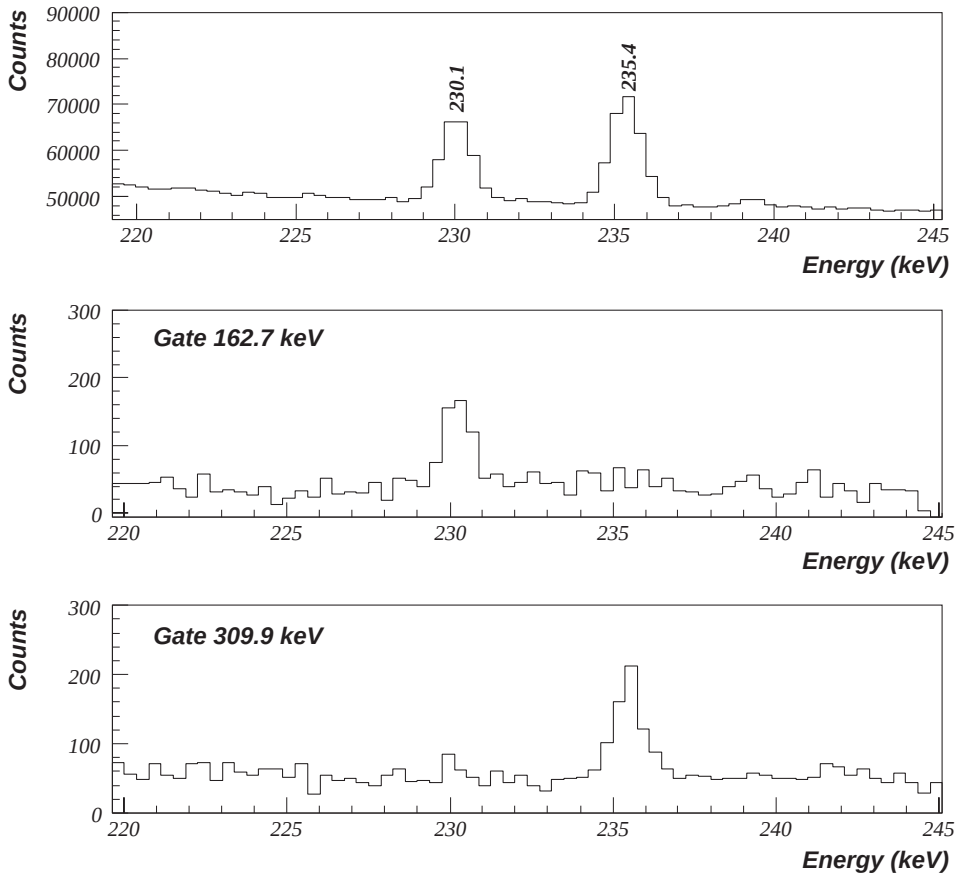

Fig. 6. Beta-gated γ-ray spectra obtained using the 70% efficiency HPGe detector placed at the collection point (bottom station). The top panel shows the integral gamma spectrum in the 220–245 keV energy interval, whereas the middle and bottom panels show spectra additionally gated with the 162.7 and 309.9 keV lines, respectively (detected in the 80% HPGe detector in the same setup). Both the connection of the 230.1 keV transition to the 162.8 keV state, and that of the 235.4 keV line to the 310.0 keV level, are clearly demonstrated.

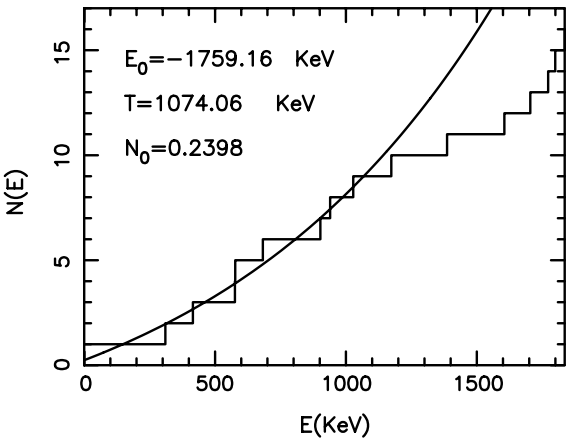

Fig. 7. Experimental integrated level density $N(E)$ and fit obtained with the constant temperature formula (see eq. (1)) [26] up to $E_x = 1173.3$ keV. All the levels with uncertain parity below this energy have been excluded from the plot.

these levels may be shifted by 101 keV due to the existence of the isomeric state, but this would not much affect their contribution to the B(GT) distribution.

In order to determine the efficiency of our decay scheme in terms of the completeness of the distribution of 1^+ states, we have analysed the cumulated level density $N(E)$ corresponding to the 1^+ and $1^{(+)}$ experimental levels, including 20 levels up to 1835.7 keV. A good description of the level density when only a few levels are known is given by the so-called *constant temperature formula* where the mean cumulated level density [26] is represented by

$$\bar{N}(E) = \exp(E - E_0)/T - \exp(-E_0/T) + N_0, \qquad (1)$$

where the parameters E_0, T and N_0 are obtained from the experimental data.

Before fitting eq. (1) to the experimental density, we can draw some preliminary conclusions using qualitative arguments. Nuclear dynamics is usually chaotic and therefore we expect the nearest-neighbour level spacing distribution to be well described by Wigner's law [27]. If this were the case, all the nearest level spacings inside a small energy window should be similar to their mean value. A visual inspection of the cumulated density shows that the spacings between 575.9 keV and 902.3 keV are either too small or too large compared with the average spacing in

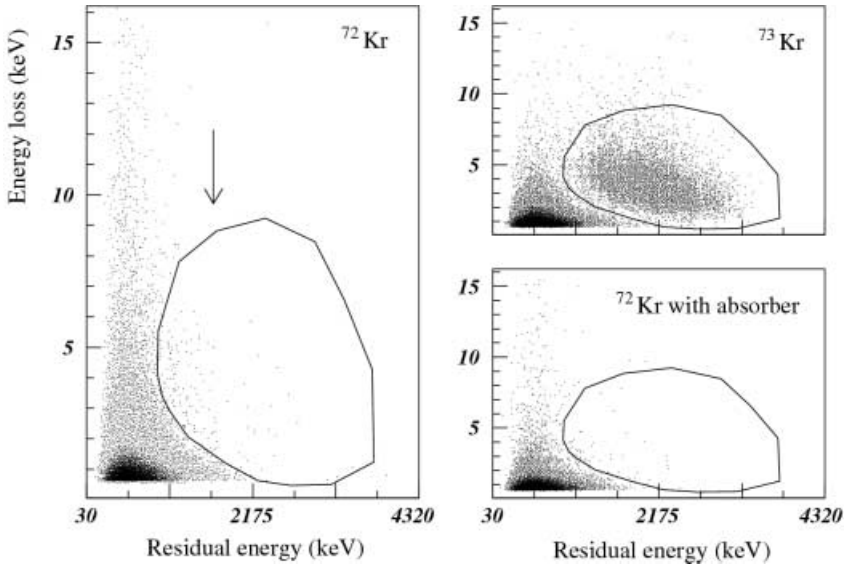

Fig. 8. Two-dimensional ΔE-E spectra obtained with the gas-Si detector telescope. Only events falling inside the region outlined by the polygon (extending from ca. 1 MeV to 3.75 MeV) were used to evaluate beta-delayed proton ratios for the two isotopes ^{72}Kr and ^{73}Kr. The upper right panel shows the ΔE-E spectrum obtained in a 30 min measurement of the ^{73}Kr, which has a well-known βp branch of $2.4(3) \times 10^{-3}$ [15]. The corresponding spectrum for ^{72}Kr, recorded during 9.5 h, is shown in the left panel. The arrow indicates the maximum βp energy for the ^{72}Kr decay. In order to investigate the contributions of beta-particles and other background sources to the spectra, a 2 h measurement with an absorber in front of the telescope was performed at the ^{72}Kr setting, as shown in the lower right panel.

this energy window. This may be due to an incorrect assignment of the parity for the three $1^{(+)}$ levels at 682.5, 708.3 and 722.2 keV. The nearest level spacings at 1173.3 and 1386.4 keV are abnormally large compared with the other spacings of similar energy. This fact suggests that some β-feeding to 1^+ levels has not been identified in the analysis.

Following these arguments we have not included the previous three $1^{(+)}$ levels in the fit of eq. (1) to the experimental density. Moreover, we have considered an energy cut-off E_x and changed its value until the agreement between the actual density $N(E)$ and the smoothed values $\bar{N}(E)$ is satisfactory for $E \in [0, E_x]$. The best fit is obtained when all the levels up to $E_x = 1173.3$ keV are considered. In this case the smooth density of eq. (1) follows the experimental staircase rather well as is shown in fig. 7 which also displays the values of the E_0, T and N_0 parameters deduced from the fit. Beyond this energy the experimental density is clearly below the exponential curve suggesting that some levels were not observed.

3.4 Search for beta-delayed particles from the ^{72}Kr decay

In order to map the whole Q_{EC} window in terms of the Gamow-Teller strength distribution, a careful search for delayed particle emission was carried out with the help of a gas-Si telescope. Independent ΔE-E particle spectra and γ-ray spectra were recorded simultaneously for about 28 h. Figure 8 displays the ΔE-E distributions for the ^{72}Kr and ^{73}Kr decays as obtained with the gas-Si telescope. On the left side of the figure one can see the distribution obtained for ^{72}Kr in normal conditions and on the bottom right side, the ΔE-E spectrum, registered with an absorber in front of the telescope. The distribution for ^{73}Kr was obtained under the same conditions as during the ^{72}Kr decay measurement. Only events falling inside the indicated polygon gate, which roughly extends from 1 MeV to 3.75 MeV, were used in the evaluation of the βp branching ratios for the two Kr isotopes. For ^{73}Kr, the obtained value is in perfect agreement with the previously published value of $2.4(3) \times 10^{-3}$ [15]. For the evaluation of the proton branching ratios in the decay of ^{72}Kr several considerations are worth of mention. Some counts are observed inside the region of interest also in the spectrum obtained with the absorber, as well as some events with an energy greater than the maximum proton energy possible for this decay ($E_{\mathrm{p,max}} = 1.69$ MeV, indicated by the arrow). These events served to evaluate the contribution of the background. A quantitative comparison has been made with the intensities of the 309.9 keV and 415.1 keV γ transitions, registered during the same time (after suitable efficiency corrections). The result of this procedure sets an upper limit of 10^{-6} for the beta-delayed proton branching ratio of ^{72}Kr. One should note the high sensitivity of the setup, as a delayed-proton branch of $3.6(7) \times 10^{-5}$ for ^{76}Sr [6] was previously measured with it, under similar experimental conditions and at an equivalent production rate.

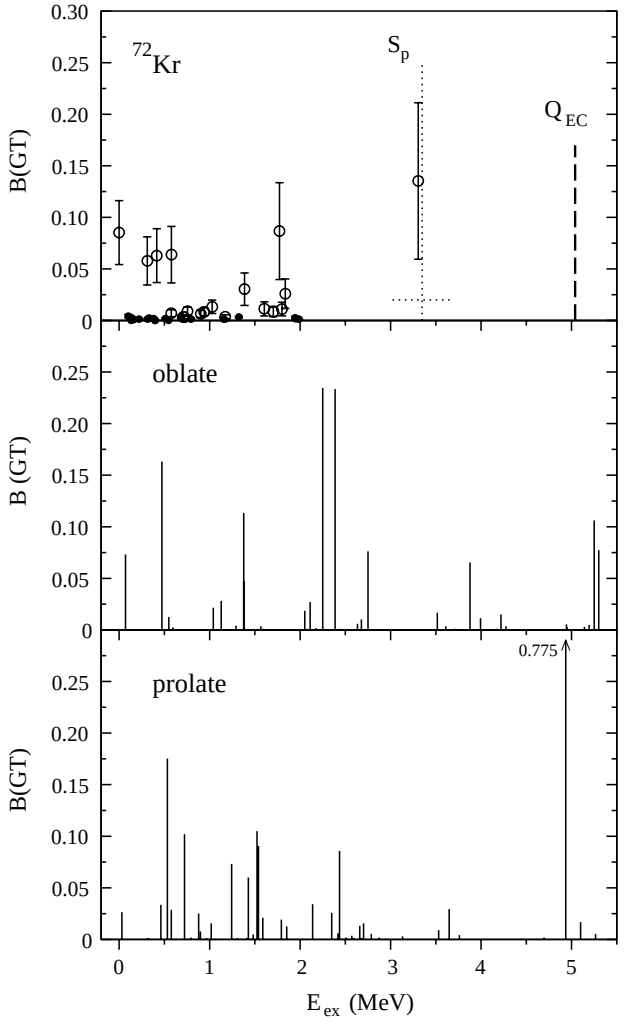

Fig. 9. The Gamow-Teller strength distribution for the β^+-EC decay of ^{72}Kr as a function of excitation energy in ^{72}Br. The experimental values in the top panel are from this work, the open circles mark the 1^+ states, the contribution from the remaining states is given by full circles. The calculated prolate and oblate B(GT) distributions are from [3]. In the prolate distribution a value of B(GT) = 0.775 is obtained for a 1^+ state near 5 MeV on ^{72}Br. The proton separation energy (S_p) and its error bar are indicated by dotted lines. The S_p value comes from systematics [13].

3.5 Gamow-Teller strength and nuclear deformation

The experimental Gamow-Teller strength distribution could only be established up to 2 MeV, as at higher energy only one level at 3.3 MeV has been firmly established. The experimental beta strength to the different levels is presented in table 4. It is of interest to compare our results with the various theoretical values obtained in the framework of mean-field calculations in terms of nuclear deformation. Such a successful comparison has already been made for ^{73}Kr and ^{75}Kr by Sarriguren *et al.* [3]. Our results are shown in fig. 9 together with the distributions of B(GT) for 1^+ states calculated by these authors [3] for prolate and oblate deformation corrected for quenching. To facilitate comparison, the B(GT) contribution from the experimentally established 1^+ states are represented by open circles and the rest of the states by full circles. It can be noticed that the high value of the Gamow-Teller (GT) strength at about 0.5 MeV excitation energy is well reproduced for both deformations. The other strong transition observed around 1.7 MeV could be related to the states found around 1.5 MeV on the basis of intensity. In the calculated distributions an obvious difference shows up in the 2–3 MeV region, where $\sum$B(GT) = 0.61 for the oblate case and 0.20 for prolate deformation. Unfortunately, we could not establish a reliable decay scheme up to this excitation energy, although we observed high-energy γ-lines in coincidence with the strongest low-energy γ-transitions, see table 2 where the coincidences are given. Recently, new data on this decay has been obtained with a total absorption NaI spectrometer and should hopefully shed light on this point.

The theoretical B(GT) strength summed from 0 to 2 MeV is 0.5 and 0.8, in the oblate and prolate cases, respectively, with the HF + QRPA approach and the SG2 Skyrme force [3]. Slightly different values were obtained by Hamamoto and Zhang [1] in the HF + TDA approximation with the SIII Skyrme interaction, namely values of 0.64 for the oblate and 0.40 in the prolate case taking into account a quenching factor of 0.6. Our value of 0.52(2) for the $\sum$B(GT) in this region cannot unambiguously assign a given deformation, but favours oblate shape for the g.s. of ^{72}Kr.

The various theoretical approaches all indicate a difference of only about 1 MeV between the oblate and prolate minima of the total energy surfaces plotted as a function of deformation. Although in all cases the oblate minimum is the deepest, the small energy difference suggests that shape coexistence should occur in ^{72}Kr. Recently, Petrovici *et al.* [28] have developed a method that gives a coherent description of ^{72}Kr and ^{74}Kr. As a result, shape coexistence and mixing at low spin have been found to be responsible for the states identified at low excitation energy. For ^{72}Kr the maximum oblate-prolate mixing was obtained for the first two 0^+ states. For the g.s. a 48% oblate/prolate mixing was found. Such a situation, which accounts for various properties of ^{72}Kr, will hinder any deformation assignment from the β-decay study. The GT strength pattern will then result from the overlap of the oblate and prolate decays with a higher number of states populated than in the case where only one of the deformations exists [1]. During the past year the $0_2^+ \longrightarrow 0_1^+$ transition in ^{72}Kr has been measured [29]. The low energy of this transition, similar to the value predicted in ref. [28], provides evidence of shape coexistence in this nucleus but the final conclusion about the composition of the ground state in terms of deformation is strongly model dependent.

4 Conclusions

This work, carried out in the framework of studies of the structure of medium-mass $N = Z$ nuclei, yields a wealth of new information on the ^{72}Br structure. Compared with

the two previous beta-decay studies our results are in qualitative agreement with those of Schmeing *et al.* [7]. Many $J^\pi = 1^+$ states have been located. The high density of 1^+ states in the first 2 MeV excitation energy is remarkable and it has been fitted with the *constant temperature formula* (eq. (1)) [26]. The comparison of theoretical and experimental level densities has allowed us to determine the excitation energy at which the number of 1^+ states is complete and therefore decide on the parities of certain levels. In our case the levels between 682.5 and 722.2 keV that are tentatively assigned as $1^{(+)}$ are not likely to have positive parity. One should note the power of the study of the cumulated level density as a tool complementary to the spin-parity determination based on the $\log f_0 t$ value. Comparing the theoretical and experimental level densities allows one to elucidate the J^π of a state when only one of the quantum numbers is unknown. The study of the nearest-neighbour level spacings indicates that the dynamics of the system at low excitation energy is not regular. However, with only the distribution of 1^+ states in a small excitation energy interval it is not possible to conclude whether it is fully chaotic.

The B(GT) distribution has been obtained for the bound states up to 2 MeV excitation energy in ^{72}Br. As for the unbound states, no β-delayed particle emission was observed down to the 10^{-6} level. The calculations in the framework of quasiparticle random phase approximation predict B(GT) distributions as well as $\sum$B(GT) values for the prolate and oblate deformation that do not differ much in the energy window under study. Therefore, no firm conclusion on the ^{72}Kr g.s. deformation can be drawn on the basis of the experimentally obtained B(GT) and $\sum$B(GT) values.

A g.s.-to-g.s. transition of allowed character has been measured for the decay $^{72}\mathrm{Kr} \rightarrow {}^{72}\mathrm{Br}$ from which $J^\pi = 1^+$ was unambiguously assigned to the ^{72}Br g.s. Calculations done in the frame of self-consistent deformed mean-field with SG2 Skyrme force and pairing favours this $J^\pi = 1^+$ assignment for a prolate nucleus ($\beta = 0.14$) with $\pi[301]3/2^- \otimes \nu[303]5/2^-$ configuration for the odd particles. The derived magnetic moment for this configuration is close to the experimental value of the g.s. magnetic moment measured by [21].

The authors are indebted to I. Hamamoto for her early calculations that supported the experimental proposal. They would also like to thank R.A. Molina, E. Moya de Guerra, A. Poves, J. Retamosa, P. Sarriguren and A. Zuker for very fruitful discussions. This work was partially supported by the Spanish Agency CICYT under contract number AEN96-1679 and AEN99-1046-C02-01, and by the French and Spanish Agreement IN2P3-CICYT.

References

1. I. Hamamoto, X.Z. Zhang, Z. Phys. A **353**, 145 (1995).
2. F. Frisk, I. Hamamoto, X.Z. Zhang, Phys. Rev. C **52**, 2468 (1995).
3. P. Sarriguren, E. Moya de Guerra, A. Escuderos, Nucl. Phys. A **658**, 13 (1999); Phys. Rev. C **64**, 0643306 (2001).
4. C. Miehé *et al.*, *Proceedings of New Facet of Spin Giant Resonances 97*, edited by H. Sakai, H. Okamura, T. Wakasa (University of Tokyo, 1998) p. 140.
5. I. Piqueras *et al.*, *Experimental Nuclear Physics in Europe 1999*, edited by B. Rubio, M. Lozano, W. Gelletly, AIP Conf. Proc. **495**, 77 (1999); Ph. Dessagne *et al.*, AIP Conf. Proc. **495**, 79 (1999).
6. A. Jokinen, C. Miehé, Hyperfine Interact. **129**, 83 (2000).
7. H. Schmeing *et al.*, Phys. Lett. B **44**, 449 (1973).
8. C.N. Davids, D.R. Goosman, Phys. Rev. C **8**, 1029 (1973).
9. W.E. Collins *et al.*, Phys. Rev. C **9**, 1457 (1974).
10. G. Garcia Bermudez *et al.*, Phys. Rev. C **25**, 1396 (1982).
11. S. Ulbig *et al.*, Z. Phys. A **329**, 51 (1988).
12. N. Fotiades *et al.*, Phys. Rev. C **60**, 57302 (1999).
13. G. Audi, A.H. Wapstra, Nucl. Phys. A **595**, 409 (1995).
14. E. Kugler, Hyperfine Interact. **129**, 23 (2000).
15. C. Miehé *et al.*, Eur. J. Phys. A **5**, 143 (1999).
16. F. Rösel *et al.*, Nucl. Data Tables. **21**, 91 (1978).
17. M.M. King, Nucl. Data Sheets **56**, 1 (1989).
18. C.N. Davids *et al.*, Bull. Am. Phys. Soc. **25**, 46 (1980).
19. R.M. Lieder, J.E. Draper, Phys. Rev. C **2**, 531 (1970).
20. J.H. Hamilton *et al.*, Phys. Rev. Lett. **12**, 239 (1974).
21. A.G. Griffiths *et al.*, Phys. Rev. C **46**, 2228 (1992).
22. P. Sarriguren *et al.*, Nucl. Phys. A **635**, 55 (1998).
23. C.J. Gallager, S.A. Moszkowski, Phys. Rev. **111**, 1282 (1958).
24. A. Bohr, B.R. Mottelson, Mat.-Fys. Medd. K. Dan. Vidensk. Selsk. **27**, no. 16 (1953).
25. E. Moya de Guerra, Phys. Rep. **138**, 293 (1986).
26. A. Gilbert, A.G.W. Cameron, Can. J. Phys. **43**, 1146 (1965).
27. E.P. Wigner, Ann. Math. **62**, 203 (1955).
28. A. Petrovici, K.W. Schmid, A. Faessler, Nucl. Phys. A **665**, 333 (2000).
29. E. Bouchez *et al.*, *Proceedings of Nuclear Physics at the Border Line 2001* (World Scientific, 2001).